A novel mutation in the NR3C1 gene associated with reversible glucocorticoid resistance

Margaux Laulhé, Emmanuelle Kuhn, Jérôme Bouligand, Larbi Amazit, Julie Perrot, Elise Lebigot, Peter Kamenický, Marc Lombès, Jérôme Fagart, Say Viengchareun, et al.

A novel mutation in the *NR3C1* gene associated with reversible glucocorticoid resistance

Margaux Laulhe[1], Emmanuelle Kuhn[2], Jérôme Bouligand[1,3], Larbi Amazit[4], Julie Perrot[1], Elise Lebigot[5], Peter Kamenický[1,6], Marc Lombès[1], Jérôme Fagart[7], Say Viengchareun[1*], Laetitia Martinerie[1,8,9*].

[1] Université Paris-Saclay, Inserm, Physiologie et Physiopathologie Endocriniennes, 94276 Le Kremlin-Bicêtre, France
[2] Service d'Endocrinologie et Métabolisme, Hôpital Pitié-Salpêtrière GHU APHP Sorbonne Université, 75013 Paris, France
[3] Service de Génétique Moléculaire, Pharmacogénétique et Hormonologie, Hôpital Bicêtre GHU APHP Paris Saclay, 94270, Le Kremlin Bicêtre, France
[4] UMS 44/ Institut Biomédical du Val de Bièvre, Université Paris-Saclay, 94276 Le Kremlin Bicêtre, France
[5] Service de Biochimie, Hôpital Bicêtre GHU APHP Paris Saclay, 94270, Le Kremlin Bicêtre, France
[6] Service d'Endocrinologie et des Maladies de la Reproduction, Hôpital Bicêtre GHU APHP Paris Saclay, 94270 Le Kremlin-Bicêtre, France
[7] CNRS UMR 7654, Ecole Polytechnique, 91120 Palaiseau, France
[8] Endocrinologie Pédiatrique, Centre de Référence Maladies Endocriniennes Rares de la Croissance et du Développement, Hôpital Universitaire Robert-Debré GHU APHP Nord, 75019 Paris, France
[9] Université Paris Cité, Faculté de Santé, UFR de Médecine, Paris, France.

[*]These authors contributed equally

Corresponding authors:
Pr Laetitia Martinerie, MD, PhD
Pediatric Endocrinology Department
CHU Robert Debré
49, boulevard Sérurier
75019, Paris
laetitia.martinerie@aphp.fr

AND

Dr Say Viengchareun, PhD
Inserm U1185
Faculté de Médecine Paris-Saclay
Bâtiment Recherche
63 rue Gabriel Péri,
94276 Le Kremlin-Bicêtre cedex, France
say.viengchareun@universite-paris-saclay.fr

Short Title: Reversible glucocorticoid resistance: case report

Keywords: adrenal adenoma, glucocorticoid resistance syndrome, glucocorticoid receptor, *NR3C1* gene.

Word Count: 4511

Abstract

Objective Glucocorticoid resistance is a rare endocrine disease caused by variants of the *NR3C1* gene encoding the Glucocorticoid Receptor (GR). We identified a novel heterozygous variant (GR_{R569Q}) in a patient with uncommon reversible glucocorticoid resistance syndrome.

Methods We performed *ex vivo* functional characterization of the variant in patient fibroblasts and *in vitro* through transient transfection in undifferentiated HEK 293T cells to assess transcriptional activity, affinity, and nuclear translocation. We studied the impact of the variant on tertiary structure of the Ligand Binding Domain (LBD) through 3D modeling.

Results The patient presented initially with an adrenal adenoma with mild autonomous cortisol secretion and undetectable ACTH levels. Six months after surgery, biological investigations showed elevated cortisol and ACTH (UFC 114 µg/24h, ACTH 10.9 pmol/L) without clinical symptoms, evoking glucocorticoid resistance syndrome. Functional characterization of the GR_{R569Q} showed decreased expression of target genes (in response to 100 nM cortisol: *SGK1* control +97% *vs.* patient +20%, $P < 0.0001$) and impaired nuclear translocation in patient fibroblasts compared to control. Similar observations were made in transiently transfected cells, but higher cortisol concentrations overcame glucocorticoid resistance. GR_{R569Q} showed lower ligand affinity (Kd GR_{WT}: 1.73 nM *vs.* GR_{R569Q}: 4.61 nM). Tertiary structure modeling suggested a loss of hydrogen bonds between H3 and the H1-H3 loop.

Conclusion This is the first description of a reversible glucocorticoid resistance syndrome with effective negative feedback on corticotroph cells regarding increased plasma cortisol concentrations due to the development of mild autonomous cortisol secretion.

Significance Statement:

We described the original case of a patient with reversible glucocorticoid resistance syndrome, initially masked by adrenal adenoma with mild autonomous cortisol secretion. We characterized a novel heterozygous variant (GR_{R569Q}) of the *NR3C1* gene, located within the Ligand Binding Domain of the Glucocorticoid Receptor (GR), responsible for a decrease in GR affinity and transactivation activity. The negative feedback of GR on the pituitary gland was restored with high cortisol concentrations despite the absence of clinical symptoms of hypercortisolism, reinforcing knowledge of the tissue specificity of glucocorticoid actions. Furthermore, our results suggest that glucocorticoid resistance syndrome should be considered in patients with adrenal incidentalomas, particularly in cases of rapid post-surgical recovery of the HPA axis.

Introduction

Glucocorticoids are steroid hormones secreted according to a circadian rhythm and in response to acute stress factors to maintain homeostasis (1,2). Glucocorticoid secretion is controlled by the Hypothalamic-Pituitary-Adrenal axis (HPA axis). The HPA axis is composed of Corticotropin-Releasing Hormone (CRH)-secreting neurons in the hypothalamus and corticotroph cells in the pituitary gland, secreting the Adrenocorticotropin Hormone (ACTH), which stimulates the synthesis of glucocorticoids in the adrenal glands. Glucocorticoids exert their functions through activation of the Glucocorticoid Receptor (GR). The GR, encoded by the *NR3C1* gene (3,4), is a nuclear receptor composed of three functional domains: the N-terminal domain (NTD), the DNA-Binding Domain (DBD), and the Ligand-Binding Domain (LBD). The glucocorticoid-bound GR is released from a multi-protein complex of heat shock proteins (Hsp90, Hsp70) and immunophilins (FKBP51, FKBP52) and translocated to the nucleus (3,5). Dimeric GR binds DNA to regulate the expression of target genes, such as *SGK1* or *TSC22D3.* The GR also acts as a monomer without binding directly to DNA but through interaction with other transcription factors such as NFκB (6).

Glucocorticoid resistance syndrome (7) is characterized by biological hypercortisolism without clinical symptoms of Cushing syndrome and the absence of negative feedback on the HPA axis (8). Chronic ACTH excess increases adrenal steroid secretion, producing androgenic and/or mineralocorticoid effects (9,10). Phenotypes of patients with glucocorticoid resistance may vary from asymptomatic to clinical manifestations of excess mineralocorticoids (hypertension, hypokalemia) or androgens (hirsutism, hypo fertility) (7,11). For example, systolic hypertension and hypokalemia due to

mineralocorticoid receptor activation in excess and elevated serum ACTH due to a lack of negative feedback on corticotroph cells were described for the first time in 1976 (10). This syndrome is generally caused by heterozygous loss-of-function variants of the *NR3C1* gene. To date, more than 30 different variants responsible for glucocorticoid resistance have been reported (7,12). The resulting receptors presented a decreased affinity for ligands (13–16) or exerted a dominant negative effect on the wild-type receptor (17). In addition, abnormalities in nuclear translocation or reduced DNA binding have also been described (18,19). Here, we present the case of a man with glucocorticoid resistance syndrome, initially masked by an adrenal incidentaloma with mild autonomous cortisol secretion that efficiently repressed ACTH secretion (20). Genetic explorations revealed a heterozygous variant of the *NR3C1* gene located in the LBD.

Materials and Methods

Ethics

The patient gave written informed consent for all genetic analyses, skin biopsy, fibroblast cultures, characterization of the mutation, and publication of the results.

Clinical and biochemical parameters

Clinical features, including CT-scan, MRI, clinical examination, biochemical parameters, and hormonal explorations, were collected from the patient's medical records during his hospital stays. Hormonal assessments (Cortisol and ACTH) were performed using immunochemiluminescence (Roche Cobas).

DNA analysis

Genomic DNA was extracted from the patient's whole blood using standard methods (QIAsymphony, QIAGEN, Hilden city, Germany). The coding regions of hGRα and hGRβ genes were amplified and sequenced as previously described (18).

Cell Culture

Human HEK 293T cells were cultured at 37°C with 5% CO_2 in DMEM (Life Technologies, Villebon-sur-Yvette, France) with 20 mM HEPES (Life Technologies), 100 UI/ml penicillin (Life Technologies), 100 µg/ml streptomycin (Life Technologies) and 10% of fetal bovine serum (Biowest, Nuaillé, France).

Fibroblasts were cultured at 37°C with 5% CO_2 in DMEM with high glucose concentration (4.5 g/L), and the addition of 20 mM HEPES, 100 UI/ml penicillin,

100 µg/ml streptomycin, and plasmocin (5 mg/L) (InvivoGen, Toulouse, France) and 15% of fetal bovine serum.

Site-directed mutagenesis

Plasmids pcDNA3-hGRα-R569Q (c.1706G>A, p.R569Q), pcDNA3-hGRα-R569K (c.1705_1706delCGinsAA, p.R569K) were obtained using the QuickChange Site-Directed Mutagenesis kit (Stratagene, La Jolla, CA) with pcDNA3-hGRα (NM_000176.2) as a template.

Transactivation assay

HEK 293T cells were transfected with plasmids expressing wild-type (WT; pcDNA3hGRα) or mutated GR (pcDNA3hGRαR569Q; 40 ng/well of 96-well plates), a reporter MMTV-luciferase plasmid (40 ng/well) and pMIRβ-galactosidase (β-gal) encoding the β-gal used to normalize luciferase activity (35 ng/well), using Lipofectamine 2000 (Life Technologies) as previously described (21). Six hours after transfection, the medium was replaced by a steroid-free medium. Twenty-four hours post-transfection, cells were treated with vehicle or increasing cortisol concentrations (0.1 to 100 nM). As previously described, Luciferase and β-gal activities were measured from cell lysates (18). Transactivation activity is expressed relative to the maximum transactivation activity obtained for GR_{WT} with 100 nM agonist concentration, arbitrarily set at 100%. EC_{50} is obtained using nonlinear regression from 6 independent experiments performed in 8 replicates. Results are expressed as median [Q1; Q2] of at least 8 replicates from 6 independent experiments. Dominant negative effect is expressed relative to the maximum transactivation activity obtained for GR_{WT} (30 ng)

with 100 nM agonist concentration, arbitrarily set at 100%. Results are expressed as median [Q1; Q2] of at least 8 replicates from 2 independent experiments.

RNA extraction and RT-qPCR

Human fibroblasts were treated with vehicle or cortisol (100 nM) for 8 h. Total RNA was extracted with the TRI Reagent® (Euromedex, Souffelweyersheim, France), according to the manufacturer's recommendations. Reverse transcription and real-time quantitative PCR (RT-qPCR) were performed as previously described (18). cDNA samples were amplified by RT-qPCR using the Quant-Studio 6 flex system (Life Technologies, Carlsbad, CA, USA). Relative expression in each sample was normalized to the internal reference *36B4* mRNA values, with control condition values arbitrarily set at 1. Results are expressed as mean±SEM (after confirming normal distribution with the d'Agostino-Pearson normality test) of at least 6 independent samples from 2 independent experiments performed in duplicates. Primers used for RT-qPCR are listed in Supplemental Data 4.

Western blot analysis

As previously described, total protein extracts were prepared from cells lysed at 4°C (22). Immunoblots were incubated overnight at 4°C with an anti-GR antibody (sc-393232, Santa Cruz, Heidelberg, Germany dilution 1/1000) with the loading control (β-actin; #A2066-.2ML, Sigma, St Quentin-Falavier, France, dilution 1/5000). Membranes were incubated at room temperature for 45 min with secondary antibodies (Pierce; Dyelight 680 #35518 or 800 #35571, Life Technologies). Bands were visualized and quantified using Odyssey®Fc, Dual-Mode Western Imagin (Li-Cor, Lincoln, NE). Results are expressed as median [Q1; Q3] of 3 to 6 independent samples from 3 independent experiments.

Hydrocortisone Binding and Scatchard plot diagram

In vitro-translated GR_{WT} and GR_{R569Q} were prepared using the rabbit reticulocyte lysate method with the TnT-T7 Quick Coupled Transcription/Translation kit (Promega, Charbonnieres-les-Bains, France) as previously described (23). Lysates were diluted 4-fold in TEGW buffer (20 mM Tris–HCl, 1 mM EDTA, 10% glycerol (v/v), 20 mM sodium tungstate pH 7.4) and incubated with increasing concentrations of [^{3}H]-Hydrocortisone (2590 GBq/mmol; Perkin Elmer, Villebon-sur-Yvette) for 4h at 4°C. Bound and unbound hydrocortisone were separated using the dextran-charcoal method (24). For an accurate calculation of the Kd values, non-specific binding (NS) was calculated using the binding-saturation model of non-linear regression with one specific site and nonspecific binding of Prism (version 10.0.2, GraphPad) and removed from each point using the formula: $B = B_{max}*X/(Kd+X) + NS*X$, where X is the ligand concentration and B_{max} the number of binding sites. The Kd and B_{max} were then calculated using the Lineweaver-Burk representation of the change in $B_{specific}$/Unbound as a function of Bspecific. Results are expressed as individual values representative of 2 independent experiments.

Immunohistochemistry, High-Throughput Microscopy (HTM) and 3D deconvolution Microscopy.

Cells were fixed with 4% paraformaldehyde for 30 min at room temperature and permeabilized for 30 min with a 0.5% solution of PBS-Triton X100. Cells were then washed 3 times with PBS and incubated for 1 h at room temperature in PBS-Tween 20 0.1% (v/v) buffer containing 5% nonfat dry milk and consecutively incubated with a mouse anti-GR antibody overnight at 4 °C (sc-393232, Santa Cruz), followed by incubation with an Alexa Fluor 555 anti-mouse secondary antibody for 30 min at room

temperature (#A32727, Life Technologies). After antibody labeling, cells were postfixed for 10 min with 4% paraformaldehyde, washed 3 times with PBS, and a nuclear counterstaining was performed with 0.5 µg/ml DAPI. HTM Images were acquired (20×/0.4 NA), analyzed, and quantified by the ArrayScan VTI imaging platform (Thermo Fisher Scientific, Asnières-sur-Seine, France) as previously described (30). Briefly, DAPI and GR fluorescence were captured using sequential acquisition to give separate image files for each. The Molecular Translocation V4 Bioapplication algorithm (vHCS Scan, version 6.3.1, Build 6586) was used to quantify the average value ratio of the nuclear intensity to the cytoplasmic intensity calculated for each selected cell per well (n > 1000 cells).

Fluorescence deconvolution microscopy was performed with Image Pro Plus AMS software (Media Cybernetics Inc, Marlow, UK) using a Mono Q Imaging Retiga 2000R Fast 1394 camera (Q Imaging Inc., Surrey, British Columbia, Canada). Cells were observed and acquired with an automated upright BX61 microscope (Olympus, Rungis, France) at 40X or 60X objective lens (1.4 NA). A z-series of focal planes were digitally imaged and deconvolved with the 3D blind iterative algorithm (Image Pro Plus AMS) to generate high-resolution images. The 3D datasets were flattened in 2D images by applying a Maximum Intensity Projection Method.

Statistical Analyses

Data are expressed as mean ± SEM when normal distribution was validated using the d'Agostino-Pearson test. Data are described as median and interquartile [Q1; Q3] if they do not follow a normal distribution. All experiments have been performed at least two times independently. We used a non-parametric Mann-Whitney test to compare two variables and a Kruskal-Wallis test to compare more than two variables. For

grouped analysis, we used multiple Mann-Whitney tests or Two-Way ANOVA test, with a Bonferroni correction, when the distribution of the variable was normal (GraphPad Prism 10.0.1, San Diego, CA). *P* values less than 0.05 were considered statistically significant. When independent experiments were pooled, the *P* value was adjusted using the Bonferroni correction.

Results

Clinical Presentation

A 45-year-old man was seen in the Endocrinology Department for diagnosis of an adrenal incidentaloma, measuring 4 cm and with low density (<10 HU) on the CT scan, as shown in Figure 1A. The CT scan was performed for the exploration of prolonged cough in the context of chronic tobacco use. The patient had been diagnosed with type 1 diabetes for 13 years; he displayed no complications despite a slightly elevated HbA1c of around 8.5%. He had no arterial hypertension, his weight was stable, and he did not display any other clinical features of Cushing syndrome. Hormonal investigations revealed cortisol-secreting adenoma: 24 h urinary free cortisol (UFC) was increased at 111 [106;116] µg/24 h (median of 2 independent assessments, N < 50 µg/24 h, Figure 1B) and ACTH was < 2.6 pmol/L (equivalent to undetectable by the assay, Figure 1C). Plasma cortisol remained elevated after the 1 mg Dexamethasone Suppression Test (DST) at 96 nmol/L (N ≤ 50 nmol/L, (25)). We did not find evidence for differential diagnosis (24 h urinary metanephrines were below normal ranges, and plasma potassium concentration was within the normal range). Given the discrepancy between clinical and biochemical parameters, they were controlled after four months. At this point, UFC was further increased (286.5 [265;308] µg/24 h), and cortisol nychthemeral rhythm was altered with elevated midnight plasma cortisol (158 nmol/L,

N < 50 nmol/L, Figure 1D); however, the patient still presented no clinical symptoms of Cushing syndrome. He was diagnosed with mild autonomous cortisol secretion (8,20,26) and, due to elevated cardiovascular risk, underwent laparoscopic surgery for unilateral adrenalectomy one month later (27). Pathological analysis was consistent with an adrenocortical adenoma measuring 40 × 27 mm with a Weiss score of 0. On the first day after surgery, plasma cortisol levels were low (49.6 nmol/L). The patient was supplemented with hydrocortisone at 20 mg/day (8). The supplementation was discontinued one month after, following a positive response to the Standard Synacthen Test (plasma cortisol rose from T0: 485 nmol/L to T60: 662 nmol/L). Approximately six months later, the patient described asthenia, anxiety, and sleep disorders. Clinical examination retrieved no symptoms of Cushing syndrome, and the abdominal CT scan found no contralateral adrenal mass. Diabetes equilibrium was stable (HbA1c 8%). New biochemical explorations revealed an elevation in the 24 h UFC (114 [101;167] µg/24 h), with no negative feedback on ACTH (10.9 [8.6;15.8] pmol/L). The post-dexamethasone (1 mg) cortisol was unsuppressed (130 nmol/L), evoking an ACTH-dependent hypercortisolism. MRI of the pituitary gland revealed no adenoma, and there was no evidence of ectopic ACTH secretion (positive response to CRH and desmopressin tests). Considering these results, we investigated glucocorticoid resistance syndrome and found a novel *NR3C1* loss-of-function heterozygous variant (Figure 2A). As the patient was asymptomatic, regular monitoring was decided. However, there was no monitoring for two years due to lost follow-up. Four years after surgery, in the context of persistent asthenia, a new hormonal assessment revealed an elevated UFC (57 [38;76] µg/24 h) with unsuppressed ACTH (17.8 [11.6;24] pmol/L). Circadian rhythm secretion of cortisol and ACTH was preserved, although with elevated values (midnight cortisol 88 nmol/L). Interestingly, 100 mg hydrocortisone

injection efficiently repressed ACTH secretion (Supplemental Data 1). These results demonstrated effective negative feedback in response to high plasma cortisol levels (2000 nmol/L after 100 mg IV hydrocortisone), explaining the patient's initial presentation of high cortisol levels associated with repressed ACTH levels. Thus, these observations suggested reversible glucocorticoid resistance in corticotroph cells.

Genetic Analysis

Sanger sequencing of the *NR3C1* gene revealed a heterozygous variant c.1706 G>A in exon 5 of *NR3C1* transcript NM_000176.3 (28) (Figure 2A, 2B). This yet unreported variation results in the substitution of Arg569 to glutamine (p.Arg569Gln) in the LBD. Unfortunately, exploration of the propositus family was not possible.

Decreased GR function in patient fibroblasts

We performed a cutaneous biopsy to obtain cultured patient fibroblasts to assess glucocorticoid sensitivity *ex vivo*. In the patient fibroblasts, both GR transcripts were expressed (Figure 2C), and total GR protein expression was not lower than in control fibroblasts (Figure 2D, E), showing that this variant does not undergo proteasomal degradation. We first studied the expression of GR target genes in response to cortisol. As the patient reversible phenotype was observed with endogenous cortisol secretion, we used cortisol in our experiments rather than the potent glucocorticoid agonist dexamethasone. Hormone-induced *SGK1* mRNA expression in response to 100 nM cortisol was lower in the patient fibroblasts compared to controls (Figure 3A, Control 1.88 ± 0.06 attomoles *vs.* Patient 1.08 ± 0.03 attomoles, $P < 0.0001$). Similarly, expression of *TSC22D3* mRNA in response to 100 nM cortisol was lower in the patient fibroblasts compared to control (Figure 3B, Control 15.02 ± 1.11 attomoles *vs.* Patient

11.59 ± 0.85 attomoles, *P* = 0.0025). As negative feedback on corticotroph cells is based on transrepression, we studied *IL6* mRNA expression, which is negatively regulated by GR through NFκB tethering (29). In basal condition, *IL6* mRNA expression is repressed only in control fibroblasts (Figure 3C, Control 1.00 ± 0.06 *vs.* Patient 3.24 ± 0.43, *P < 0.0001*). In response to 100 nM cortisol, *IL6* mRNA expression is decreased similarly in patient and control fibroblasts (Figure 3C, Control 0.20 ± 0.02 *vs.* Patient 0.40 ± 0.02, NS), suggesting a rescue of transrepression activity under high cortisol concentrations. Further, as the GR LBD also contains a Nuclear Localization Signal (NLS), we investigated the nuclear translocation of GR in fibroblasts. It is worth noting that both the wild-type (GR_{WT}) and the variant receptor (GR_{R569Q}) are expressed in the patient fibroblasts and detected by the same antibody (Figure 2C). Cells were stimulated for one hour with increasing cortisol concentrations (from 0 to 100 nM). Nuclear translocation was quantified using automated high-throughput microscopy by measuring the nuclear-to-cytoplasmic ratio as previously described (30). As shown in Figure 3D, GR_{WT} is exclusively nuclear when cells are stimulated with 10 nM cortisol. In contrast, it was both nuclear and cytoplasmic in the patient fibroblasts (Figure 3E, at 10 nM Cortisol nuclear/cytoplasmic ratio Control 3.92 ± 0.07 *vs.* Patient 2.87 ± 0.16, *P* < 0.0001). These data are consistent with a gene-specific decreased GR activity in patient cells. These data confirmed that GR_{R569Q} activity is reduced in response to cortisol, consecutively to a defect in nuclear translocation.

The GR_{R569Q} is associated with a reduced affinity for cortisol.

To assess the specific transcriptional activity of GR_{R569Q} compared to GR_{WT}, we designed expression vectors comprising either GR_{R569Q} or GR_{WT} that we transiently transfected in HEK 293T cells. We used HEK 293T cells because endogenous GR

expression is almost null. We first showed that GR_{R569Q} transactivated the MMTV-Luc reporter gene in a dose-dependent manner, but with a higher half-maximal effective concentration (EC_{50}) compared to the GR_{WT} (Figure 4A, EC_{50} for GR_{WT}: 0.87 [0.30;0.95] nM *vs.* EC_{50} for GR_{R569Q}: 1.91 [1.73;5.07], P = 0.0011). When we transfected equal amount of GR_{WT} and GR_{R569Q}, we observed a dominant negative effect on transcriptional activity in the presence of 10 nM cortisol (Figure 4B, GR_{WT} 70.50 [67.25;84.50] *vs* $GR_{WT/R569Q}$ 45.50 [40;55.50], $P < 0.001$) that was rescued with 100 nM cortisol (Figure 4B, GR_{WT} 104.5 [92.75;109.75] *vs* $GR_{WT/R569Q}$ 113.5 [100.75;131], P = 0.196). In transfected HEK 293T cells, GR_{R569Q} is localized in the cytoplasm even at 10 nM cortisol compared to cells transfected with the $GR_{WT,}$ where GR is mainly nuclear. These results were confirmed by automated high-throughput microscopy (Figure 4D, N/C at 10 nM cortisol for GR_{WT} 3.04 ± 0.04 *vs* N/C at 10 nM cortisol for GR_{R569Q} 1.76 ± 0.04, $P < 0.0001$). At 100 nM cortisol, the nuclear/cytoplasmic ratio appeared to be less different (Figure 4D, N/C at 100 nM cortisol for GR_{WT} 3.98 ± 0.07 *vs* N/C at 100 nM cortisol for GR_{R569Q} 3.64 ± 0.07, $P < 0.0001$). These results are consistent with reversible glucocorticoid resistance in presence of high concentrations of cortisol. As the genetic variation is located within the LBD, we hypothesized that a decreased affinity for cortisol may be responsible for the phenotype. GR-expressing lysates were incubated with increasing concentrations of [^{3}H]-hydrocortisone, and the dissociation constants were measured at equilibrium. As expected, GR_{R569Q} showed a reduced affinity for cortisol (Figure 4E, GR_{WT} 1.73 nM (IC95 0.69;0.46) vs. GR_{R569Q} 4.61 nM (IC95 0.28;0.14), $P < 0.0001$).

Three-dimensional model of the GR-LBD

Arg569 is located within the helix H3 of the LBD, which is a determinant that allows ligand binding (Figure 5A) (29). The crystal structure of the GR-LBD bound to dexamethasone and chaperone proteins revealed that Arg569 establishes two strong hydrogen bonds with the main carbonyl chain of Tyr545 and Ala546 located within the loop connecting the Helix H1 to Helix H3 (PDB 7KRJ, Figure 5B) (5). As shown in Figure 5C, substituting Arg569 with a shorter glutamine may result in the loss of these hydrogen bonds that may destabilize the LBD structure even without a direct interaction with the ligand. In the co-chaperones complex of the unliganded structure of the GR-LBD, Arg569 also connects the H1-H3 loop at Ser551 and Val552 through hydrogen bonds, whereas Gln569 is unable to maintain such bonds (Supplemental Data 2). Interestingly, those amino acids are implicated in physiological glucocorticoid resistance in Guinea Pig (32) through decreased GR ligand-binding activity *via* interaction with FKBP51 and FKBP52 co-chaperone proteins. To determine whether these modifications are responsible for the elevated EC_{50} observed with GR_{R569Q}, we mutated Arg569 to a lysine (GR_{R569K}). This basic amino acid is closer to arginine and may reestablish the hydrogen bonds. Our results showed that the reverse variant, GR_{R569K} exhibited an improved transactivation capacity (Supplemental Data 3A and 3B, EC_{50} GR_{WT} 0.93 [0.89;1.00], GR_{R569Q} 2.10 [1.76;4.83], GR_{R569K} 1.60 [1.29;1.69], P=0.015) but without complete reversion, suggesting a more complex function for Arg569.

Discussion

We identified a novel missense variant within the GR LBD associated with reversible glucocorticoid resistance. Primary glucocorticoid resistance syndrome is characterized by hypercortisolemia with normal or elevated ACTH without corresponding clinical signs of Cushing syndrome (7). In this case, the patient presented with an adrenal adenoma with mild autonomous cortisol secretion. The association between adrenal hyperplasia or adenoma and glucocorticoid resistance has already been described but is usually associated with normal or elevated ACTH levels (18,22,31). HPA axis stimulation, due to impaired negative feedback, can lead to adrenal hyperplasia, as suggested in mice with GR haploinsufficiency (33). Further, the Muta-GR study estimated *NR3C1* loss-of-function variants in 5 of 100 patients with adrenal hyperplasia associated with either biological hypercortisolism and/or hypertension without clinical symptoms of Cushing syndrome (34). The five patients presented with variants in the DBD (GR_{R469X} and GR_{R477S}) and the LBD (GR_{R491S}, GR_{Q501H}, and GR_{L672P}). Among these, four presented with biological evidence of glucocorticoid resistance. Some of the variants were extensively described in different studies (18,22), showing either the absence of DNA binding (GR_{R469X} and GR_{R477S}) or increased proteasomal degradation (GR_{L672P}). The authors concluded that *NR3C1* variants should be investigated in patients presenting with adrenal hyperplasia associated with low aldosterone and potassium levels and biological hypercortisolism. Although our results reinforce the hypothesis of elevated prevalence of *NR3C1* variants in adrenal hyperplasia, utilization of those criteria would not have permitted to diagnose the patient as aldosterone levels and kaliemia were both normal.

Other cases of glucocorticoid resistance have been described in association with adrenal incidentaloma. The first case, published by Zhu et *al.*, was a 56-year-old patient with a right adrenal incidentaloma with elevated ACTH and UFC levels persisting after surgery (35). The patient displayed a heterozygous variant (GR_{T556I}) within the fifth exon of the *NR3C1* gene. Nicolaides et al. showed a decreased affinity (50%), transcriptional activity (50%), and nuclear translocation of the variant, but no evidence for a dominant negative effect (31). The variant GR_{T556I} exhibited a defective interaction of its AF-2 domain with GRIP1 and an increased transrepressive activity. The second patient with left adrenal incidentaloma and glucocorticoid resistance was described by our team and displayed a heterozygous variant corresponding to a tyrosine-to-cysteine substitution at amino acid 478 (GR_{Y478C}) within the DBD. Functional characterization of this variant revealed a decreased transactivation, decreased nuclear translocation, and DNA binding without any dominant negative effect or decreased affinity (22). None of these patients presented effective negative feedback, as ACTH levels were within the normal range at diagnosis. In these cases, glucocorticoid resistance-related HPA axis activation may have been responsible for adrenal incidentaloma. In our patient's case, glucocorticoid resistance related to HPA axis activation may have led to autonomous cortisol secretion. Subsequently, high plasma cortisol levels may have led to effective negative feedback on the HPA axis, which might explain why glucocorticoid resistance was not initially diagnosed. Hypothesis of two unrelated events is possible but seemed unlikely as plasma ACTH levels were repressed after 100 mg hydrocortisone injection, showing effective negative feedback on the corticotroph cells (Supplemental Data 1). Symptomatic glucocorticoid resistance syndrome treatment is based on mineralocorticoid-sparing synthetic glucocorticoids, such as dexamethasone. The aim is to suppress the HPA

axis activity and reduce ACTH secretion and adrenal stimulation (36), suggesting that a high concentration of glucocorticoid agonists may restore glucocorticoid negative feedback. Decreased sensitivity of the receptor, which can be overcome with high concentrations of agonists, is commonly observed in variations within the LBD of nuclear receptors such as androgen receptor (AR), mineralocorticoid receptor (MR), or vitamin D receptor (37). Interestingly, urinary-free cortisol levels evolved as a mirror image of plasma ACTH levels in the case described herein. Currently, UFC above 150 µg/24h is associated with a decrease in plasma ACTH levels, suggesting that endogenous hypercortisolism is sufficient to achieve effective negative feedback.

In vitro characterization of the *NR3C1* heterozygous variant GR_{R569Q} showed a lower transactivation activity with an increased EC_{50}. Transactivation activity results from several steps that the variant may have impaired. First, GR_{R569Q}'s affinity for hydrocortisone was 1.5 times lower than GR_{WT} (Figure 4E). The mutated arginine is localized within the LBD on helix H3 (Figure 5A). While helix H3 is a Ligand Binding Pocket (LBP) component, there is no direct interaction between Arg569 and the ligand as it is orientated outside the LBP (34,35). Modeling of the GR-LBD bound to dexamethasone (PDB 7KRJ, Figure 5) showed that Arg569 makes hydrogen bonds with Tyr545 and Ala546 on the H1-H3 loop. The hydrogen bond with Tyr545 is conserved in antagonist and agonistic conformation of the LBD (5,38–40) but not in unliganded conformation. In the latter, Arg569 makes hydrogen bonds with Ser551 and Val552 in H1-H3 loop, suggesting a role for Arg569 in the conformational change of the unliganded-LBD to the liganded-LBD. These amino acids are involved in glucocorticoid resistance observed in guinea pigs (41). Guinea pig exhibits physiological glucocorticoid resistance with elevated cortisol levels due to changes in amino acids within the LBD (42) and, more precisely, within the H1-H3 loop.

Modification of the H1-H3 loop results in altered interactions with chaperone proteins FKBP51 and FKBP52 through a particular 3D-conformation of the LBD, conferring glucocorticoid resistance (32). FKBP51 and FKBP52 regulate GR and other steroid receptors affinity for agonists and nuclear translocation (43,44). Consistent with these data, we showed decreased nuclear translocation in patient fibroblasts and transiently transfected cells (Figure 3D, E, Figure 4B, C). Therefore, it would be interesting to study interactions of GR_{R569Q} with FKBP52 and FKBP51.

Further, we observed a dominant-negative effect of GR_{R569Q} on GR_{WT} transactivation capacity (Figure 4B). Indeed, transfection of both GRs in equal amounts led to a decreased transcriptional activity compared to GR_{WT} alone, consistent with the results obtained in the patient's fibroblasts. However, glucocorticoid resistance was not reversible with high cortisol levels depending on the gene, suggesting gene-specific cortisol sensitivity associated with this variant. The gene-specific impact of GR variants has been described concerning other well-known variants, such as N363S polymorphism (45) and MR resistance syndrome (46). Furthermore, mice $GR^{dim/dim}$ with a reduced capacity of GR dimerization exhibited gene- and tissue-specific alteration in glucocorticoid signaling pathways (47,48). Tissue-specific GR regulation may explain why the patient did not present clinical symptoms of hypercortisolism, even when HPA axis negative feedback was efficient, and plasma ACTH levels were low, mirroring high cortisol levels. Further this discrepancy may be explained by the different mechanisms of GR signaling. The differential impact of *NR3C1* loss-of-function variants on transactivation and transrepression activity has already been described, but the molecular mechanism remains unclear (31,51). At the pituitary level, glucocorticoid-dependent transrepression of the ACTH precursor, the Pro-opiomelanocortin *(POMC)* gene, depends in part on inhibition of Nur77 transactivation

activity through tethering (49,50). Unfortunately, we were not able to study GR_{R569Q} impact in corticotroph cells, nor did we characterize the variant *in vivo* in a mice model. Nevertheless, we showed that transrepression of the NFκB target gene, *IL6*, is rescued in the patient fibroblasts in response to 100 nM cortisol. This suggests that transrepression of GR target-genes through tethering mechanisms may be restored at plasma cortisol concentrations lower than those necessary to regain full GR transactivation through direct DNA-binding.

In conclusion, we described a novel heterozygous variant of the *NR3C1* gene associated with glucocorticoid resistance. To our knowledge, this is the first description of a patient with constitutive glucocorticoid resistance initially masked by adrenocortical adenoma with autonomous cortisol secretion. Thus, it emphasizes the question, previously addressed in the Muta-GR study, of the prevalence of GR variants in patients with adrenal incidentaloma and mild autonomous cortisol secretion, particularly in the case of rapid post-surgical recovery of the HPA axis (34). Our functional studies support the critical role of H3 and the H1-H3 loop in the ligand binding. Finally, this is the first demonstration of a reversible glucocorticoid resistance with effective negative feedback on corticotroph cells secondary to mild autonomous cortisol secretion, which brings new insight into tissue-specific glucocorticoid regulation of target genes.

Data Availability

The data supporting this study's findings are available upon request from the corresponding author. The data are not publicly available due to privacy or ethical restrictions.

Acknowledgments

The authors are grateful to A. Blin and P. Tandabany for technical assistance.

Funding Statement

This research program was supported by Inserm (Institut national de la santé et de la recherche) and Université Paris-Saclay. Margaux Laulhé was the recipient of an SFEDP (Société Francaise d'Endocrinologie et de Diabétologie Pédiatrique) price during her Master 2 Degree. During her PhD program, she benefits from financial support from ITMO Cancer of Aviesan (Institut Thématique Multi-Organisme Cancer de l'Alliance nationale pour les sciences de la vie et de la santé) within the framework of 2021-2030 Cancer Control Strategy, on funds administered by Inserm.

Author contribution

Conceptualization: Margaux Laulhé, Emmanuelle Kuhn, Jérôme Bouligand, Larbi Amazit, Julie Perrot, Peter Kamenicky, Jérôme Fagart, Marc Lombès, Say Viengchareun and Laetitia Martinerie

Formal analysis: Margaux Laulhé, Larbi Amazit, Jérôme Fagart, Say Viengchareun and Laetitia Martinerie

Funding acquisition: Say Viengchareun and Laetitia Martinerie

Investigation: Margaux Laulhé, Emmanuelle Kuhn, Julie Perrot, Jerome Bouligand, Elise Lebigot, Jérôme Fagart, Say Viengchareun and Laetitia Martinerie

Methodology: Margaux Laulhé, Emmanuelle Kuhn, Julie Perrot, Jérôme Fagart, Larbi Amazit, Say Viengchareun and Laetitia Martinerie

Project administration: Say Viengchareun and Laetitia Martinerie

Resources: Elise Lebigot, Jérôme Bouligand; Jérôme Fagart

Validation: Margaux Laulhé, Emmanuelle Kuhn, Jérôme Bouligand, Larbi Amazit, Julie Perrot, Peter Kamenicky, Marc Lombès, Jérôme Fagart, Say Viengchareun and Laetitia Martinerie

Writing-original draft: Margaux Laulhé, Larbi Amazit, Jérôme Fagart, Say Viengchareun, and Laetitia Martinerie

Writing-review & editing: Margaux Laulhé, Emmanuelle Kuhn, Jérôme Bouligand, Larbi Amazit, Julie Perrot, Elise Lebigot, Peter Kamenicky, Marc Lombès, Jérôme Fagart, Say Viengchareun and Laetitia Martinerie

Ethic Declaration

Written consent for genetic testing and additional written consent for the publication were obtained from the patient.

Conflict of Interest

The authors declare no conflict of interest.

Figures Legend

Figure 1. Clinical and biological phenotype

A) CT-scan figuring a right adrenal incidentaloma of 44x27 mm with low attenuation (3 UH) (White Arrow).

B) Graphic representation of ACTH (pmol/L, solid line) throughout the years. Data are expressed as median [Q1;Q3] from at least two values whenever possible. The normal range is figured in grey. HC: Hydrocortisone supplementation.

C) Graphic representation of 24 h Urinary Free-Cortisol (µg/24h, dashed line) throughout the years. Data are expressed as median [Q1;Q3] from at least two values whenever possible. The normal range is figured in grey. HC: Hydrocortisone supplementation.

D) Graphic representation of midnight plasma cortisol (nmol/L, dashed line) throughout the years. Data are expressed as median [Q1;Q3] from at least two values whenever possible. The normal range is figured in grey. HC: Hydrocortisone supplementation.

Figure 2. A novel heterozygous missense variant located in the LBD

A) Schematic representation of the Glucocorticoid Receptor with the localization of the missense variation from gene to protein (NTD: N-Terminal Domain, DBD: DNA Binding Domain, LBD: Ligand Binding Domain).

B) Chromatograph of the genomic DNA extracted from patient fibroblasts. The heterozygous variation is figured with a black arrow.

C) Chromatograph of the complementary DNA extracted from patient fibroblasts. Expression of both alleles is figured by the double-peak shown by a black arrow.

D) Protein expression of GR in patient fibroblasts (90 kDa). The lysate and protein extract of the transfected cells were analyzed by SDS-PAGE. GR proteins were detected by

Western Blot analyses using mouse antibody targeting hGRα N-terminal domain. β-actin was used as a loading control. Representative image of 3 independent experiments is shown.

E) Quantification of protein level. Specific bands were quantified by Odyssey FC, Dual Mode Western Imaging. Results are expressed as median [Q1; Q2] and normalized to β-actin loading, with control condition values arbitrarily set at 1. Data are expressed from individual samples from 3 independent experiments. Statistical analysis was performed using Mann Whitney t-test with Bonferroni correction, **** $P < 0.0001$.

Figure 3. Expression of the GR_{R569Q} is associated with impaired transactivation and delayed nuclear translocation but effective transrepression.

A) Relative mRNA expression of GR target gene, *SGK1,* measured by RT-qPCR. Control and patient fibroblasts were incubated with 0 or 100 nM concentration of cortisol for 8 h. *SGK1* mRNA expression, expressed in attomoles, was normalized with *36B4* mRNA, and expressed relative to the minimum expression obtained for GR_{WT} with no agonist, arbitrarily set at 1. Data are expressed as mean ± SEM from 6 replicates of 2 independent experiments. Statistical significance was calculated with 2-way ANOVA test with Bonferroni correction, ****$P < 0.0001$.

B) Relative mRNA expression of GR target gene, *TSC22D3,* measured by RT-qPCR. Control and patient fibroblasts were incubated with 0 or 100 nM concentration of cortisol for 8 h. *TSC22D3* mRNA expression, expressed in attomoles, was normalized with *36B4* mRNA, expressed relative to the minimum expression obtained for GR_{WT} with no agonist, arbitrarily set at 1. Data are expressed as mean ± SEM from 6 replicates of 2 independent experiments. Statistical significance was calculated with 2-way ANOVA test with Bonferroni correction, ** $P = 0.0025$.

C) Relative mRNA expression of GR target gene *IL6* measured by RT-qPCR. Control and patient fibroblasts were incubated with 0 or 100 nM concentration of cortisol for 8 hours. *IL6* mRNA expression expressed in attomoles was normalized with *36B4* mRNA, and expressed relative to the minimum expression obtained for GR_{WT} with no agonist, arbitrarily set at 1. Data expressed as mean±SEM from 6 replicates of 2 independent experiments. Statistical significance was calculated with 2-way ANOVA test with Bonferroni correction, ****$P < 0.0001$.

D) Control and patient fibroblasts were incubated with 0 to 100 nM cortisol for 1 h. Cells were fixed and processed for immunochemistry as described in the Materials and Methods section—representative images of the subcellular localization of GR (red). A *z*-series of focal planes was digitally imaged and deconvolved using ImageProPlusAMS iterative algorithm to generate high-resolution images. DAPI staining delineates the nuclei (blue). GR nuclear localization is figured in the Merged panel (pink); scale bar represents 100 µM.

D) Automated high-throughput microscopy quantification of the molecular translocation of GR_{WT} and GR_{R569Q}. Cells were treated as described in C), and fluorescence acquisition was performed with the Array Scan VTI fluorescent microscope. The translocation index (nucleo-cytoplasmic ratio) represents the average ratio of the nuclear fluorescence intensity to the cytoplasmic fluorescence intensity calculated for each transfected cell (n>1000). Data expressed as mean ± SEM from each field (n = 50) of 2 independent experiments. Statistical significance was calculated with the 2-way ANOVA test with Bonferroni correction, * P = 0.001, ****$P < 0.0001$.

Figure 4. Decreased transcription activity of the GR_{R569Q} can be overcome with high concentrations of cortisol

A) HEK 293T cells were transiently transfected with GR_{WT} or GR_{R569Q} encoding plasmids (40 ng), a reporter luciferase plasmid pMMTV-Luc (40 ng) and pMIRβ gal (35 ng). Cells were treated 24 h with increasing cortisol concentrations (0.1 to 100 nM). Transactivation activity is expressed relatively to the maximum transactivational activity obtained for GR_{WT} with 100 nM agonist concentration, arbitrarily set at 100%. EC_{50} is obtained using nonlinear regression from 6 independent experiments performed in 8 replicates. Statistical significance was calculated with the Mann-Whitney t-test, ** P = 0,0011.

B) HEK 293T cells were transiently transfected with either 30 ng of GR_{WT} or GR_{R569Q} encoding plasmid alone, or 30 ng of both, associated with a reporter luciferase plasmid pMMTV-Luc (40 ng) and pMIRβ gal (35 ng). Cells were treated for 24 h with increasing cortisol concentrations (0, 10 or 100 nM). Transactivation activity was expressed relatively to the maximum transactivational activity obtained for 30 ng GR_{WT} at 100 nM cortisol, arbitrarily set at 100%). Data expressed as median[Q1; Q3] from 8 replicates of 2 independent experiments. Statistical significance was calculated with the Multiple Mann-Whitney test with Bonferroni correction, **** $P < 0.0001$.

C) COS-7 cells were transiently transfected with GR_{WT} or GR_{R569Q} encoding plasmids (400 ng). Transfected cells were incubated with 0 to 100 nM cortisol for 1 h and 24 h after transfection. Cells were fixed and processed for immunochemistry as described in the Materials and Methods section—representative images of the subcellular localization of GR (red). A *z*-series of focal planes was digitally imaged and deconvolved using ImageProPlusAMS iterative algorithm to generate high-resolution images. DAPI staining delineates the nuclei (blue). GR nuclear localization is figured in the Merged panel (pink); scale bar represents 50 µM.

D) Automated high-throughput microscopy quantification of the molecular translocation of GR_{WT} and GR_{R569Q}. Cells were treated as described in C), and fluorescence acquisition was performed with the Array Scan VTI fluorescent microscope. The translocation index (nucleo-cytoplasmic ratio) represents the average ratio of the nuclear fluorescence intensity to the cytoplasmic fluorescence intensity calculated for each transfected cell (n>1000). Nuclear cytoplasmic ratio was expressed as fold change from GR_{WT} without cortisol, arbitrarily set at 1. Data expressed as mean ± SEM from each field (n = 50) from 2 independent experiments. Statistical significance was calculated with the 2-way ANOVA test with Bonferroni correction, ****$P < 0.0001$.

E) Scatchard analysis of hydrocortisone binding to GR_{WT} and GR_{R569Q}. I*n vitro* expressed GR_{WT} or GR_{R569Q} were incubated with increasing concentrations of [^{3}H]-hydrocortisone (0.5 to 70 nM) for 4h at 4°C. Bound and unbound ligands were separated by the dextran-charcoal method; after removing the nonspecific component, the evolution of the bound/unbound as a function of the amount bound was plotted, and the dissociation constant at equilibrium (Kd) was calculated from the slope obtained with linear regression. Statistical analysis of the slopes showed that the difference between the slopes is significant (P<0.0001) representative data of 2 independent experiments.

Figure 5. Three-dimensional model of the ligand-bound GR-LBD.

A) Picture showing the overall organization of the agonist-bound GR-LBD (PDB 7KRJ). The α-helices and beta-sheets are depicted as ribbons and arrows, respectively. Selected residues are shown with their carbon, oxygen, and nitrogen atoms colored in white, red, and blue, respectively. Dexamethasone is shown with its carbon, oxygen, and fluoride atoms colored in violet, red, and pale blue, respectively.

B) Focus on the hydrogen-bound network involving Arg569 from helix H3 and Tyr545 and Ala546 from Loops 1-3.

C) Focus showing the loss of hydrogen bonds after substitution of Arg569 to Gln569.

Supplemental Data 1. Restoration of an effective negative feedback on ACTH secretion.

A) Graphical representation of ACTH (pmol/L, solid line) secretion in response to 100 mg hydrocortisone injection four years post-adrenalectomy. Normal range is figured in light grey.

Supplemental Data 2. Three-dimensional model of the unliganded GR-LBD.

A) Picture showing the overall organization of the apo GR-LBD (PDB 7KW7). The α-helices and beta-sheets are depicted as ribbons and arrows, respectively. Selected residues are shown with their carbon, oxygen, and nitrogen atoms colored in white, red, and blue, respectively.

B) Focus on the hydrogen bound network involving Arg569 from helix H3 and Ser551 and Val552 from Loop 1-3.

C) Focus showing the loss of hydrogen bonds after substitution of Arg569 to Gln569.

Supplemental Data 3. Transactivation activity of the GR_{R569K}

A) HEK 293T cells were transiently transfected with GR_{WT} or GR_{R569Q} or GR_{R569K} encoding plasmids (40 ng), a reporter luciferase plasmid pMMTV-Luc (40 ng) and pMIRβ gal (35 ng). Cells were treated 24 h with increasing cortisol concentrations (0 to 100 nM). Transactivation activity was expressed relatively to the maximum transactivational

activity obtained for GR_{WT} at 100 nM, arbitrarily set at 100%. Data are representative of 3 experiments performed in 8 replicates. Statistical significance was calculated with 2-way ANOVA test with Bonferroni correction, ****P < 0,0001.

B) HEK 293T cells were transiently transfected with GR_{WT} or GR_{R569Q} or GR_{R569K} encoding plasmids, a reporter luciferase plasmid pMMTV-Luc and pMIRβ gal. Cells were treated 24h with increasing cortisol concentrations (0.1 to 100 nM). Transactivation activity is expressed relatively to the maximum transactivational activity obtained for GR_{WT} with 100 nM agonist concentration, arbitrarily set at 100%. EC_{50} is obtained using nonlinear regression from 3 independent experiments performed in 8 replicates. Statistical significance was calculated with the Kruskal Wallis test, *P = 0,015.

Supplemental Data 4. Target genes primers

All primer sequences are shown from 5' to 3'.

References

1. Whirledge S, DeFranco DB. Glucocorticoid Signaling in Health and Disease: Insights From Tissue-Specific GR Knockout Mice. Endocrinology. 2018 Jan 1;159(1):46–64.

2. Rhen T, Cidlowski JA. Antiinflammatory action of glucocorticoids--new mechanisms for old drugs. N Engl J Med. 2005 Oct 20;353(16):1711–23.

3. Kadmiel M, Cidlowski JA. Glucocorticoid receptor signaling in health and disease. Trends Pharmacol Sci. 2013 Sep;34(9):518–30.

4. Hollenberg SM, Weinberger C, Ong ES, Cerelli G, Oro A, Lebo R, et al. Primary structure and expression of a functional human glucocorticoid receptor cDNA. Nature. 1985 Dec 19;318(6047):635–41.

5. Wang RYR, Noddings CM, Kirschke E, Myasnikov AG, Johnson JL, Agard DA. Structure of Hsp90-Hsp70-Hop-GR reveals the Hsp90 client-loading mechanism. Nature. 2022 Jan;601(7893):460–4.

6. Ratman D, Vanden Berghe W, Dejager L, Libert C, Tavernier J, Beck IM, et al. How glucocorticoid receptors modulate the activity of other transcription factors: a scope beyond tethering. Mol Cell Endocrinol. 2013 Nov 5;380(1–2):41–54.

7. Nicolaides NC, Charmandari E. Primary Generalized Glucocorticoid Resistance and Hypersensitivity Syndromes: A 2021 Update. Int J Mol Sci. 2021 Oct 7;22(19):10839.

8. Fleseriu M, Auchus R, Bancos I, Ben-Shlomo A, Bertherat J, Biermasz NR, et al. Consensus on diagnosis and management of Cushing's disease: a guideline update. Lancet Diabetes Endocrinol. 2021 Dec;9(12):847–75.

9. Reul JM, Sutanto W, van Eekelen JA, Rothuizen J, de Kloet ER. Central action of adrenal steroids during stress and adaptation. Adv Exp Med Biol. 1990;274:243–56.

10. Vingerhoeds AC, Thijssen JH, Schwarz F. Spontaneous hypercortisolism without Cushing's syndrome. J Clin Endocrinol Metab. 1976 Nov;43(5):1128–33.

11. Vitellius G, Trabado S, Bouligand J, Delemer B, Lombès M. Pathophysiology of Glucocorticoid Signaling. Annales d'Endocrinologie. 2018 Jun;79(3):98–106.

12. Paragliola RM, Costella A, Corsello A, Urbani A, Concolino P. A Novel Pathogenic Variant in the N-Terminal Domain of the Glucocorticoid Receptor, Causing Glucocorticoid Resistance. Mol Diagn Ther. 2020 Aug 1;24(4):473–85.

13. Charmandari E, Raji A, Kino T, Ichijo T, Tiulpakov A, Zachman K, et al. A Novel Point Mutation in the Ligand-Binding Domain (LBD) of the Human Glucocorticoid Receptor (hGR) Causing Generalized Glucocorticoid Resistance: The Importance of the C Terminus of hGR LBD in Conferring Transactivational Activity. The Journal of Clinical Endocrinology & Metabolism. 2005 Jun;90(6):3696–705.

14. Chrousos GP, Vingerhoeds A, Brandon D, Eil C, Pugeat M, DeVroede M, et al. Primary cortisol resistance in man. A glucocorticoid receptor-mediated disease. J Clin Invest. 1982 Jun;69(6):1261–9.

15. Nader N, Bachrach BE, Hurt DE, Gajula S, Pittman A, Lescher R, et al. A novel point mutation in helix 10 of the human glucocorticoid receptor causes generalized glucocorticoid resistance by disrupting the structure of the ligand-binding domain. J Clin Endocrinol Metab. 2010 May;95(5):2281–5.

16. Nicolaides NC, Charmandari E, Chrousos GP, Kino T. Recent advances in the molecular mechanisms determining tissue sensitivity to glucocorticoids: novel mutations, circadian rhythm and ligand-induced repression of the human glucocorticoid receptor. BMC Endocr Disord. 2014 Dec;14(1):71.

17. Trebble P, Matthews L, Blaikley J, Wayte AWO, Black GCM, Wilton A, et al. Familial glucocorticoid resistance caused by a novel frameshift glucocorticoid receptor mutation. J Clin Endocrinol Metab. 2010 Dec;95(12):E490-499.

18. Bouligand J, Delemer B, Hecart AC, Meduri G, Viengchareun S, Amazit L, et al. Familial Glucocorticoid Receptor Haploinsufficiency by Non-Sense Mediated mRNA Decay, Adrenal Hyperplasia and Apparent Mineralocorticoid Excess. Reitsma PH, editor. PLoS ONE. 2010 Oct 22;5(10):e13563.

19. Karl M, Lamberts SW, Koper JW, Katz DA, Huizenga NE, Kino T, et al. Cushing's disease preceded by generalized glucocorticoid resistance: clinical consequences of a novel, dominant-negative glucocorticoid receptor mutation. Proc Assoc Am Physicians. 1996 Jul;108(4):296–307.

20. Pelsma ICM, Fassnacht M, Tsagarakis S, Terzolo M, Tabarin A, Sahdev A, et al. Comorbidities in mild autonomous cortisol secretion and the effect of treatment: systematic review and meta-analysis. Eur J Endocrinol. 2023 Oct 17;189(4):S88–101.

21. Vitellius G, Delemer B, Caron P, Chabre O, Bouligand J, Pussard E, et al. Impaired 11β-Hydroxysteroid Dehydrogenase Type 2 in Glucocorticoid-Resistant Patients. J Clin Endocrinol Metab. 2019 Nov 1;104(11):5205–16.

22. Vitellius G, Fagart J, Delemer B, Amazit L, Ramos N, Bouligand J, et al. Three Novel Heterozygous Point Mutations of NR3C1 Causing Glucocorticoid Resistance. Hum Mutat. 2016 Aug;37(8):794–803.

23. Fagart J, Hillisch A, Huyet J, Bärfacker L, Fay M, Pleiss U, et al. A new mode of mineralocorticoid receptor antagonism by a potent and selective nonsteroidal molecule. J Biol Chem. 2010 Sep 24;285(39):29932–40.

24. Fagart J, Seguin C, Pinon GM, Rafestin-Oblin ME. The Met852 residue is a key organizer of the ligand-binding cavity of the human mineralocorticoid receptor. Mol Pharmacol. 2005 May;67(5):1714–22.

25. Fassnacht M, Tsagarakis S, Terzolo M, Tabarin A, Sahdev A, Newell-Price J, et al. European Society of Endocrinology clinical practice guidelines on the management of adrenal incidentalomas, in collaboration with the European Network for the Study of Adrenal Tumors. European Journal of Endocrinology. 2023 Jul 20;189(1):G1–42.

26. Prete A, Subramanian A, Bancos I, Chortis V, Tsagarakis S, Lang K, et al. Cardiometabolic Disease Burden and Steroid Excretion in Benign Adrenal Tumors : A Cross-Sectional Multicenter Study. Ann Intern Med. 2022 Mar;175(3):325–34.

27. Bancos I, Prete A. Approach to the Patient With Adrenal Incidentaloma. J Clin Endocrinol Metab. 2021 Oct 21;106(11):3331–53.

28. Freeman PJ, Hart RK, Gretton LJ, Brookes AJ, Dalgleish R. VariantValidator: Accurate validation, mapping, and formatting of sequence variation descriptions. Hum Mutat. 2018 Jan;39(1):61–8.

29. Hudson WH, Vera IMS de, Nwachukwu JC, Weikum ER, Herbst AG, Yang Q, et al. Cryptic glucocorticoid receptor-binding sites pervade genomic NF-κB response elements. Nat Commun. 2018 Apr 6;9(1):1337.

30. Amazit L, Le Billan F, Kolkhof P, Lamribet K, Viengchareun S, Fay MR, et al. Finerenone Impedes Aldosterone-dependent Nuclear Import of the Mineralocorticoid Receptor and Prevents Genomic Recruitment of Steroid Receptor Coactivator-1. J Biol Chem. 2015 Sep 4;290(36):21876–89.

31. Nicolaides NC, Skyrla E, Vlachakis D, Psarra AMG, Moutsatsou P, Sertedaki A, et al. Functional characterization of the hGRαT556I causing Chrousos syndrome. Eur J Clin Invest. 2016 Jan;46(1):42–9.

32. Cluning C, Ward BK, Rea SL, Arulpragasam A, Fuller PJ, Ratajczak T. The helix 1-3 loop in the glucocorticoid receptor LBD is a regulatory element for FKBP cochaperones. Mol Endocrinol. 2013 Jul;27(7):1020–35.

33. Michailidou Z, Carter RN, Marshall E, Sutherland HG, Brownstein DG, Owen E, et al. Glucocorticoid receptor haploinsufficiency causes hypertension and attenuates hypothalamic-pituitary-adrenal axis and blood pressure adaptions to high-fat diet. FASEB J. 2008 Nov;22(11):3896–907.

34. Vitellius G, Trabado S, Bouligand J, Hoeffel C, Mantel AG, Delemer B, et al. Résultats du PHRC National muta-GR : prévalence des mutations NR3C1 dans l'hyperplasie bilatérale des surrénales. Annales d'Endocrinologie. 2017 Sep 1;78(4):216.

35. Zhu H juan, Dai Y fei, Wang O, Li M, Lu L, Zhao W gang, et al. Generalized glucocorticoid resistance accompanied with an adrenocortical adenoma and caused by a novel point mutation of human glucocorticoid receptor gene. Chin Med J (Engl). 2011 Feb;124(4):551–5.

36. Tatsi C, Xekouki P, Nioti O, Bachrach B, Belyavskaya E, Lyssikatos C, et al. A novel mutation in the glucocorticoid receptor gene as a cause of severe glucocorticoid resistance complicated by hypertensive encephalopathy. J Hypertens. 2019 Jul;37(7):1475–81.

37. Achermann JC, Schwabe J, Fairall L, Chatterjee K. Genetic disorders of nuclear receptors. Journal of Clinical Investigation. 2017 Apr 3;127(4):1181–92.

38. Bledsoe RK, Montana VG, Stanley TB, Delves CJ, Apolito CJ, McKee DD, et al. Crystal structure of the glucocorticoid receptor ligand binding domain reveals a novel mode of receptor dimerization and coactivator recognition. Cell. 2002 Jul 12;110(1):93–105.

39. He Y, Yi W, Suino-Powell K, Zhou XE, Tolbert WD, Tang X, et al. Structures and mechanism for the design of highly potent glucocorticoids. Cell Res. 2014 Jun;24(6):713–26.

40. Kauppi B, Jakob C, Färnegårdh M, Yang J, Ahola H, Alarcon M, et al. The three-dimensional structures of antagonistic and agonistic forms of the glucocorticoid receptor ligand-binding domain: RU-486 induces a transconformation that leads to active antagonism. J Biol Chem. 2003 Jun 20;278(25):22748–54.

41. Zuckerman SH, Bendele AM. Regulation of serum tumor necrosis factor in glucocorticoid-sensitive and -resistant rodent endotoxin shock models. Infect Immun. 1989 Oct;57(10):3009–13.

802 42. Keightley MC, Curtis AJ, Chu S, Fuller PJ. Structural determinants of cortisol resistance in the guinea
803 pig glucocorticoid receptor. Endocrinology. 1998 May;139(5):2479–85.

804 43. Vandevyver S, Dejager L, Libert C. On the Trail of the Glucocorticoid Receptor: Into the Nucleus
805 and Back: Nuclear Transport of Glucocorticoid Receptor. Traffic. 2012 Mar;13(3):364–74.

806 44. Kirschke E, Goswami D, Southworth D, Griffin PR, Agard DA. Glucocorticoid receptor function
807 regulated by coordinated action of the Hsp90 and Hsp70 chaperone cycles. Cell. 2014 Jun
808 19;157(7):1685–97.

809 45. Jewell CM, Cidlowski JA. Molecular Evidence for a Link between the N363S Glucocorticoid
810 Receptor Polymorphism and Altered Gene Expression. J Clin Endocrinol Metab. 2007
811 Aug;92(8):3268–77.

812 46. Fernandes-Rosa FL, Hubert EL, Fagart J, Tchitchek N, Gomes D, Jouanno E, et al. Mineralocorticoid
813 Receptor Mutations Differentially Affect Individual Gene Expression Profiles in
814 Pseudohypoaldosteronism Type 1. The Journal of Clinical Endocrinology & Metabolism. 2011 Mar
815 1;96(3):E519–27.

816 47. Timmermans S, Verhoog NJD, Van Looveren K, Dewaele S, Hochepied T, Eggermont M, et al. Point
817 mutation I634A in the glucocorticoid receptor causes embryonic lethality by reduced ligand
818 binding. J Biol Chem. 2022 Feb;298(2):101574.

819 48. Jewell CM, Scoltock AB, Hamel BL, Yudt MR, Cidlowski JA. Complex human glucocorticoid receptor
820 dim mutations define glucocorticoid induced apoptotic resistance in bone cells. Mol Endocrinol.
821 2012 Feb;26(2):244–56.

822 49. Martens C, Bilodeau S, Maira M, Gauthier Y, Drouin J. Protein-protein interactions and
823 transcriptional antagonism between the subfamily of NGFI-B/Nur77 orphan nuclear receptors and
824 glucocorticoid receptor. Molecular Endocrinology (Baltimore, Md). 2005 Apr;19(4):885–97.

825 50. Reichardt HM, Kaestner KH, Tuckermann J, Kretz O, Wessely O, Bock R, et al. DNA binding of the
826 glucocorticoid receptor is not essential for survival. Cell. 1998 May 15;93(4):531–41.

827 51. Nicolaides NC, Roberts ML, Kino T, Braatvedt G, Hurt DE, Katsantoni E, et al. A novel point mutation
828 of the human glucocorticoid receptor gene causes primary generalized glucocorticoid resistance
829 through impaired interaction with the LXXLL motif of the p160 coactivators: dissociation of the
830 transactivating and transreppressive activities. J Clin Endocrinol Metab. 2014 May;99(5):E902-907.

831

A

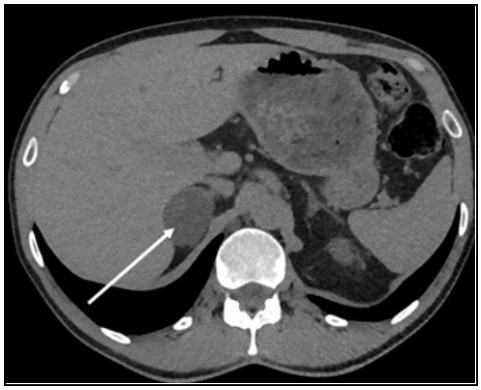

B

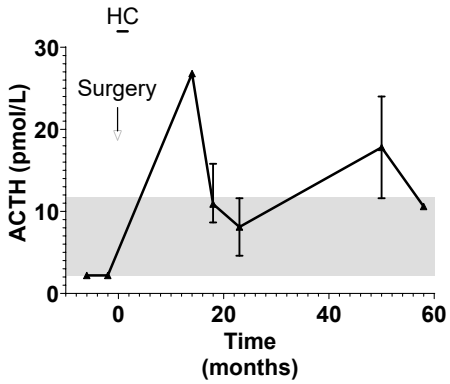

C

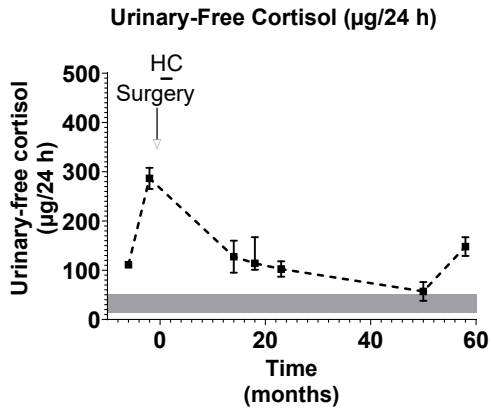

D

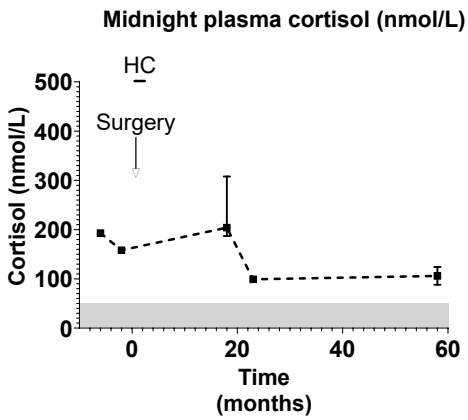

Figure 1. Clinical and biological phenotype

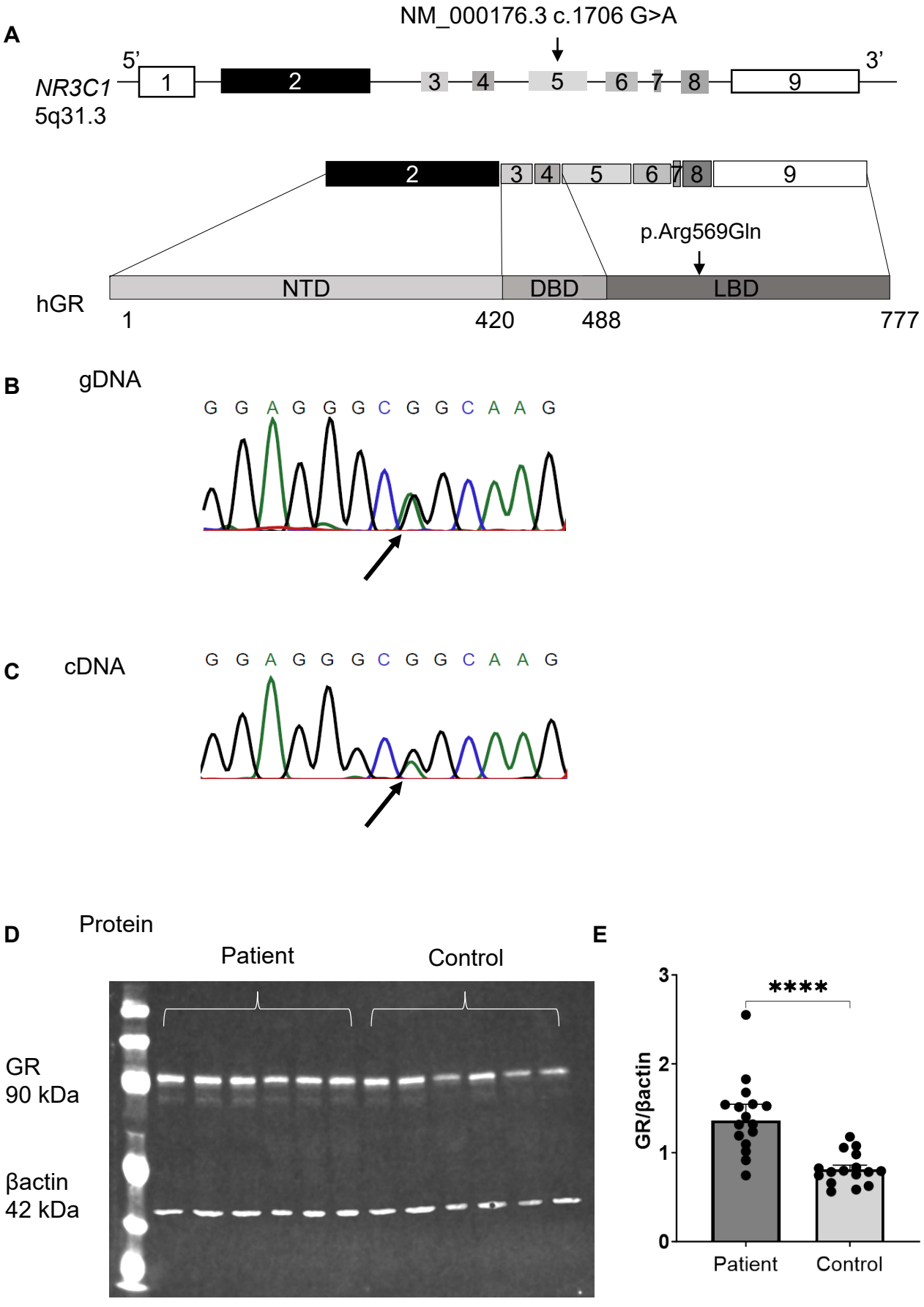

Figure 2. A novel heterozygous missense variant located in the GR LBD

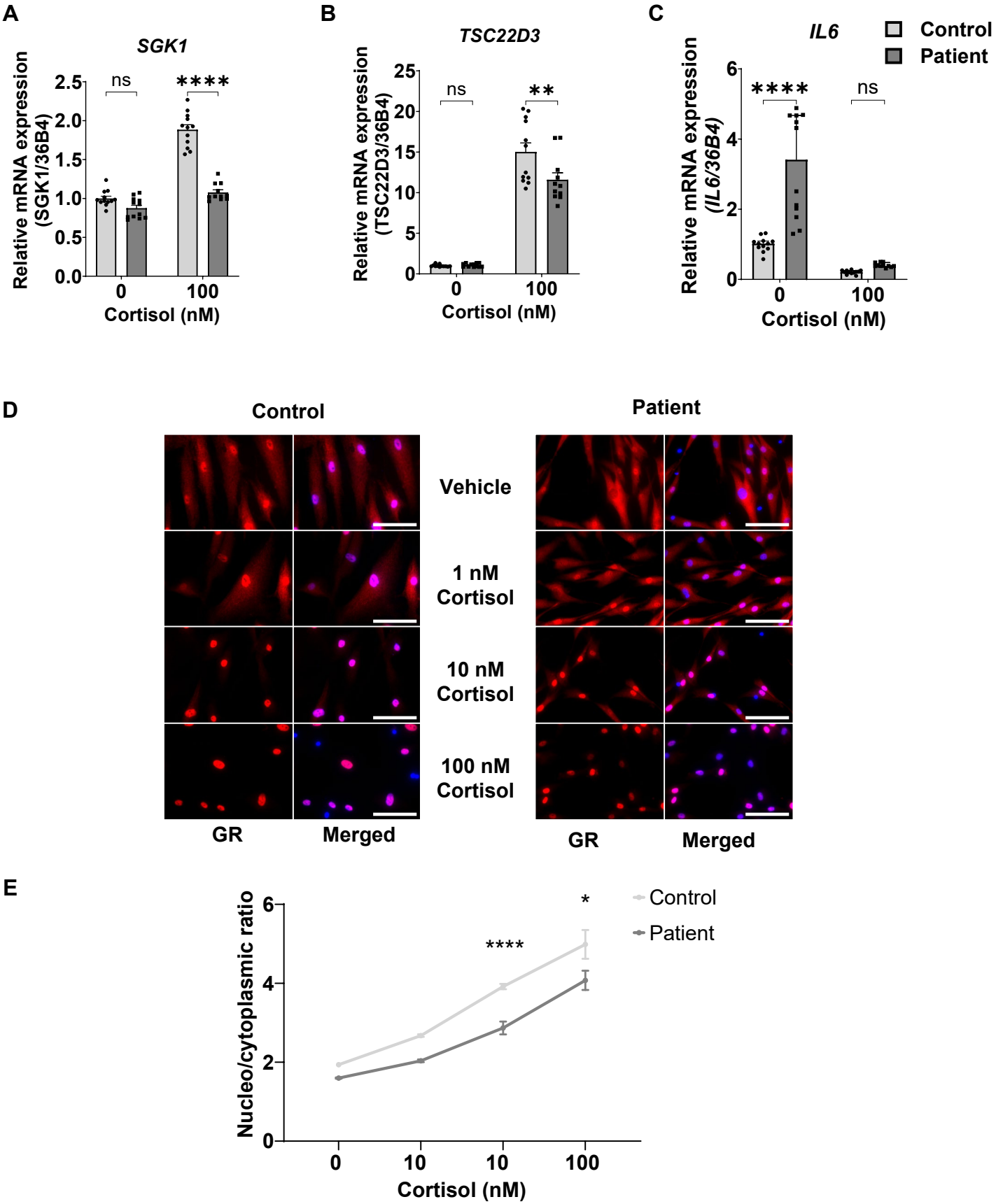

Figure 3. Expression of the GR_{R569Q} is associated with impaired transactivation and delayed nuclear translocation but effective transrepression

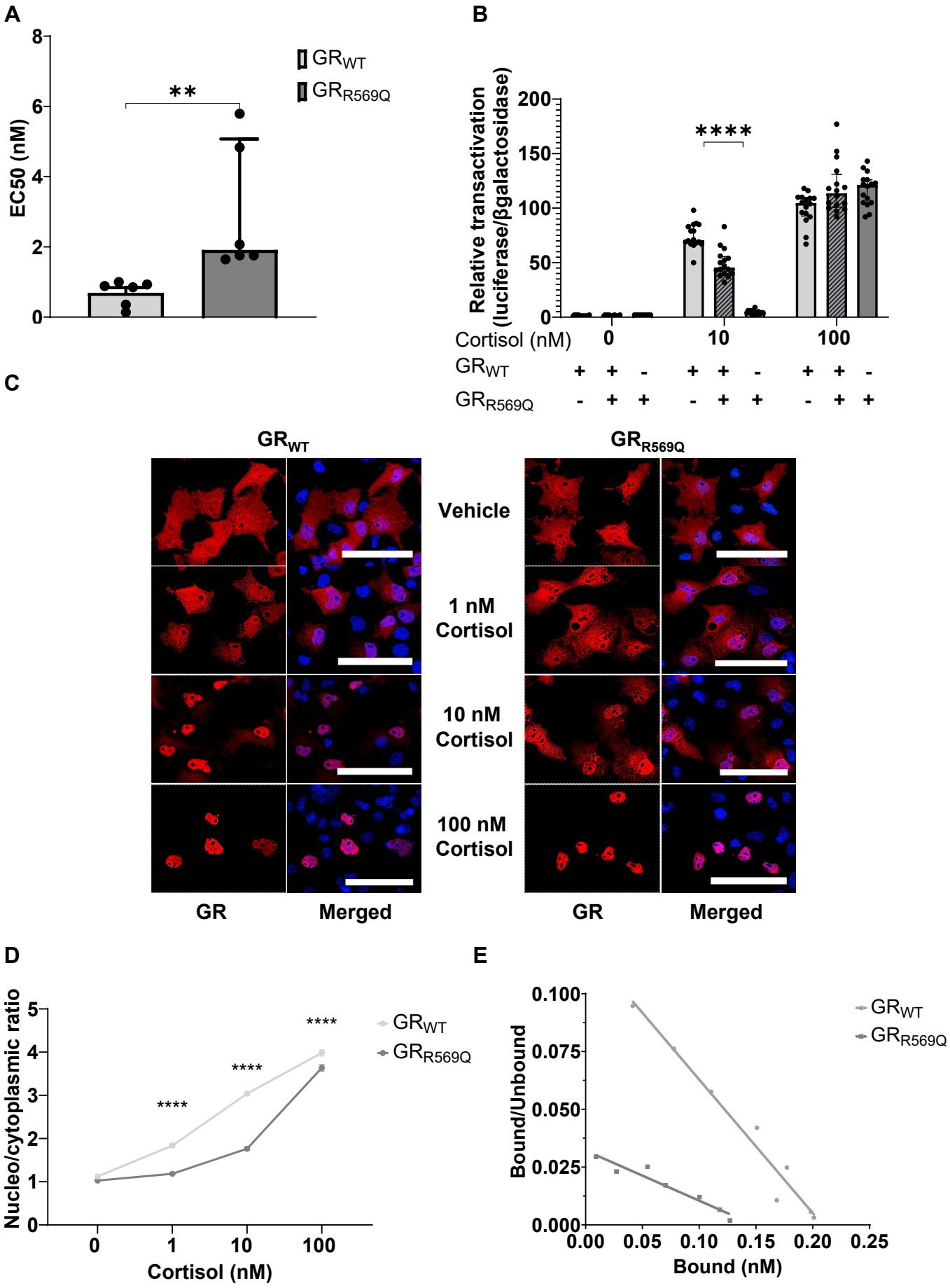

Figure 4. Decreased transcription activity of the GR_{R569Q} can be overcome with high concentrations of cortisol

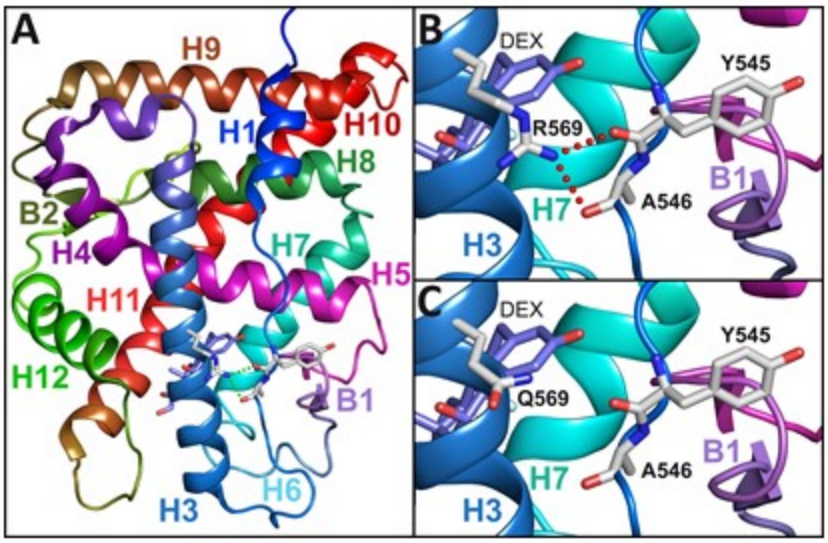

Figure 5. Three-dimensional model of the ligand-bound GR-LBD

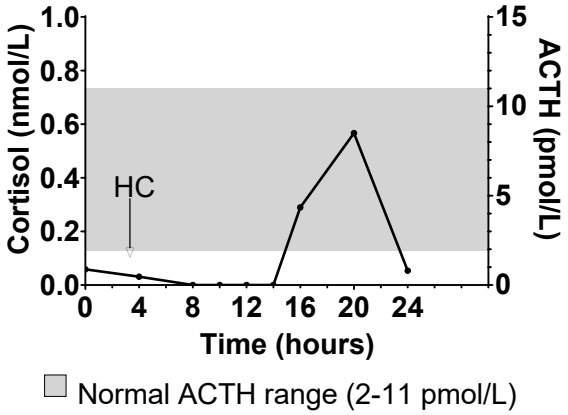

Supplemental Data 1. Restoration of an effective negative feedback on ACTH secretion

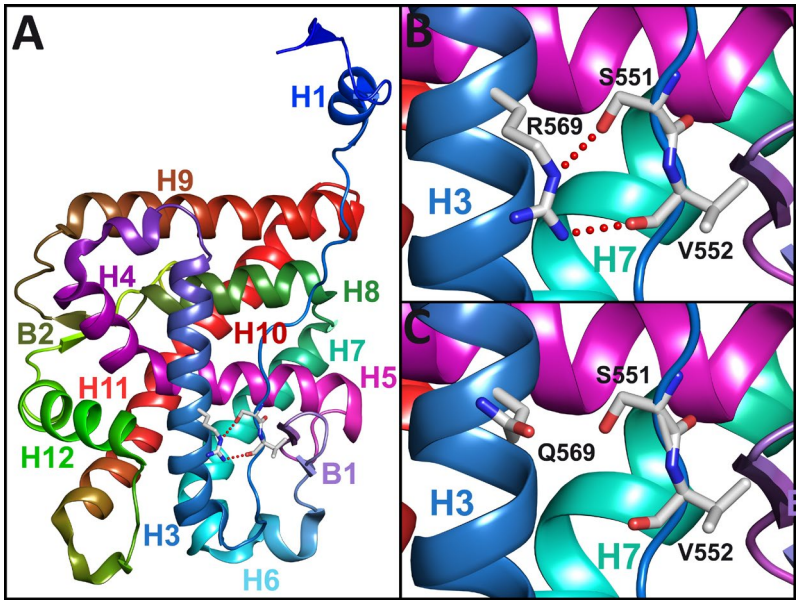

Supplemental Data 2. Three-dimensional model of the unliganded GR-LBD

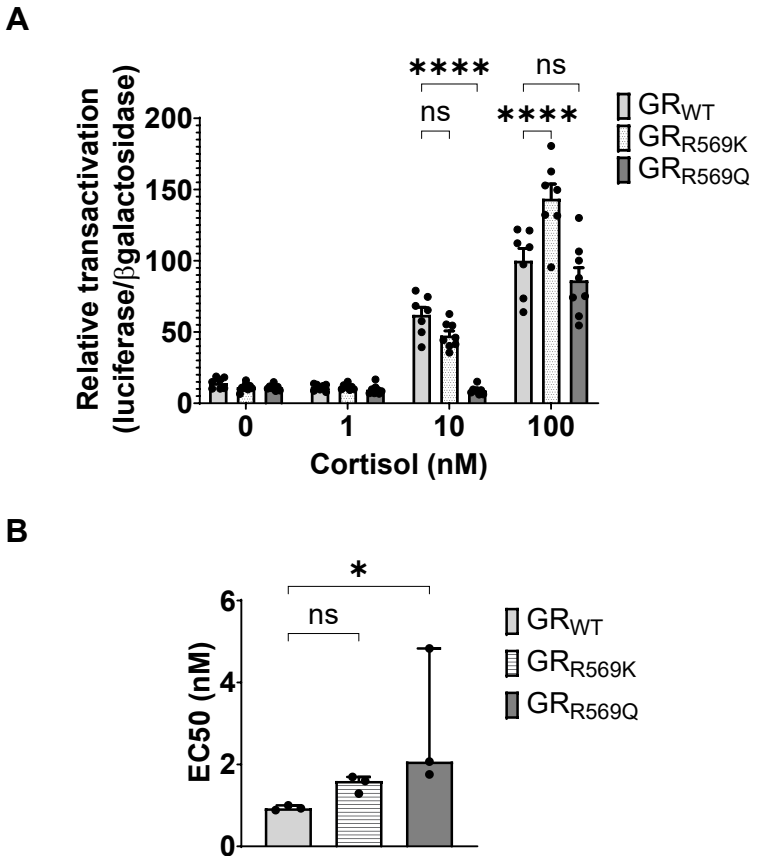

Supplemental Data 3. Transactivation activity of the GR_{R569K}

GENE	Primer sequence
h36B4 _F	CCC-ATT-CTA-TCA-TCA-ACG-GGT-ACA-A
h36B4 _R	CAG-CAA-GTG-GGA-AGG-TGT-AAT-CC
hTSC22D3 _F	TCC-TGA-AGG-AGC-AGA-TCC-GA
hTSC22D3 _R	TCT-TCA-GGG-CTC-AGA-CAG-GA
hSGK1 _F	GTC-GCA-ATT-CTC-ATC-GCT-TTC
hSGK1 _F	CTT-CAG-GGT-GTT-TGC-ATG-CAT
hIL6 _F	AGG-GCT-CTT-CGG-CAA-ATG-TA
hIL6 _R	TGC-CCA-GTG-GAC-AGG-TTT-CT

Supplemental Data 4. Target genes primers